Molecular Vision 2017; 23:395-406 <http://www.molvis.org/molvis/v23/395>
Received 12 February 2017 | Accepted 30 June 2017 | Published 3 July 2017

Genome-wide retinal transcriptome analysis of endotoxin-induced uveitis in mice with next-generation sequencing

Yiguo Qiu,[1] Peng Yu,[1] Ru Lin,[1] Xinyu Fu,[1] Bingtao Hao,[2] Bo Lei[3,1]

(The first two authors contributed equally to this study.)

[1]Department of Ophthalmology, the First Affiliated Hospital of Chongqing Medical University, Chongqing Key Laboratory of Ophthalmology, Chongqing Eye Institute, Chongqing, China; [2]Cancer Research Institute, Southern Medical University, Guangzhou, China; [3]Henan Provincial People's Hospital and People's Hospital of Zhengzhou University, Henan Eye Institute, Henan Eye Hospital, Zhengzhou, China

Purpose: Endotoxin-induced uveitis (EIU) is a well-established mouse model for studying human acute inflammatory uveitis. The purpose of this study is to investigate the genome-wide retinal transcriptome profile of EIU.
Methods: The anterior segment of the mice was examined with a slit-lamp, and clinical scores were evaluated simultaneously. The histological changes in the posterior segment of the eyes were evaluated with hematoxylin and eosin (H&E) staining. A high throughput RNA sequencing (RNA-seq) strategy using the Illumina Hiseq 2500 platform was applied to characterize the retinal transcriptome profile from lipopolysaccharide (LPS)-treated and untreated mice. The validation of the differentially expressed genes (DEGs) was analyzed with real-time PCR.
Results: At the 24th hour after challenge, the clinical score of the LPS group was significantly higher (3.83±0.75, mean ± standard deviation [SD]) than that of the control group (0.08±0.20, mean ± SD; $p<0.001$). The histological evaluation showed a large number of inflammatory cells infiltrated into the vitreous cavity in the LPS group compared with the control group. A total of 478 DEGs were identified with RNA-seq. Among these genes, 406 were upregulated and 72 were downregulated in the LPS group. Gene Ontology (GO) enrichment showed three significantly enriched upregulated terms. Twenty-one upregulated and seven downregulated pathways were remarkably enriched by Kyoto Encyclopedia of Genes and Genomes (KEGG) pathway enrichment. Eleven inflammatory response–, complement system–, fibrinolytic system–, and cell stress–related genes were validated to show similar results as the RNA-seq.
Conclusions: We first reported the retinal transcriptome profile of the EIU mouse with RNA-seq. The results indicate that the abnormal changes in the inflammatory response–, complement system–, fibrinolytic system–, and cell stress–related genes occurred concurrently in EIU. These genes may play an important role in the pathogenesis of EIU. This study will lead to a better understanding of the underlying mechanisms and shed light on discovering novel therapeutic targets for ocular inflammation.

Uveitis is a common inflammatory ocular disease that compromises the vision of patients and even causes blindness within the working population worldwide [1]. Several etiologies that could lead to uveitis have been proposed, including trauma, infection, and autoimmune disease [2]. Uveitis can act either as an isolated intraocular inflammation or as a part of systemic autoimmune diseases [3,4].

Currently, the conventional treatment for uveitis includes topical or systemic administration of corticosteroids, nonsteroidal anti-inflammatory drugs (NSAIDs), and immunosuppressive agents. Despite these available treatments, some patients do not respond well to these drugs; consequently, the inflammation becomes refractory or chronic. Even if the drugs are highly efficacious to patients, long-term application may bring about numerous adverse effects, including cataract, glaucoma, metabolic disorders, and even liver or kidney failure [5-7]. Therefore, identification of novel and effective therapeutic targets with fewer side effects for the treatment of uveitis is highly desired.

Involving inflammation of the uveal tract, endotoxin-induced uveitis (EIU) is a widely used animal model that shares many clinical and histological characteristics with human acute infectious uveitis. EIU can be induced via a single systemic or local injection of lipopolysaccharide (LPS) [7]. The process of inflammatory response induced by LPS is well understood. LPS stimulation activates Toll-like receptor 4 (TLR4) to initiate the cellular inflammatory pathways, including the transcription factors nuclear factor (NF)-κB and activator protein (AP)-1, and results in the release of cytokines and chemokines and increased expression of adhesion molecules [8-10].

Correspondence to: Bo Lei, People's Hospital of Zhengzhou University, Henan Provincial People's Hospital, Henan Eye Institute, Henan Eye Hospital, Zhengzhou, China; Phone: 86 37165580903; FAX: 86 37165580903; email: bolei99@126.com

Identification of the abnormally changed genes or molecular pathways may discover potential therapeutic targets, which can be facilitated with high-throughput systems analyses, particularly at the transcriptome levels. The transcriptome is an integrated set of transcripts at a specific stage or under a given physiologic condition [11]. Transcriptome analysis is one of the approaches that aims to identify the genetic variations of a disease and investigate its pathogenesis. Next-generation sequencing (NGS) technology has launched a new era of tremendous potential and applications in genomic and transcriptomic analyses [12,13].

RNA-sequencing with NGS (RNA-seq) provides a comprehensive evaluation and quantification of all subtypes of RNA molecules expressed in a cell or tissue [14]. RNA-seq technology has many advantages compared with earlier technologies. First, it is highly reproducible and has a much greater dynamic range than the microarray analysis. Second, RNA-seq can detect transcripts expressed at low levels [15]. Within the constraints of the coverage depth, RNA-seq can measure the level of any transcripts present in the library and permit the identification of unannotated transcripts, different splice variants, and non-coding RNAs [14,16-19]. Therefore, RNA-seq is expected to reveal a better representation of the transcriptome. Moreover, with a steady reduction in the costs of NGS, RNA-seq is now emerging as a method of choice for comprehensive transcriptome profiling.

Accumulating evidence indicates that genome-wide characterization of the retinal transcriptome is essential to understanding the cell development, physiology, as well as disease of the eye [20-22]. Thus, RNA-seq technology may have the potential to reveal comprehensive and detailed information about the transcriptome changes during a disease. In the present study, we used NGS-based RNA-seq analysis to investigate the retinal transcriptome profile of EIU and control mice. We identified a series of differentially expressed genes. This study illustrates that RNA-seq offers a more complete, more accurate, and faster approach for comparative and comprehensive analysis of retinal transcriptomes in EIU and may open up new avenues for discovering new therapeutic targets for ocular inflammation.

METHODS

Ethics statement: The study was performed according to the ARVO Statement for the Use of Animals in Ophthalmic and Vision Research. The protocols were approved by the Ethics Committee of the First Affiliated Hospital of Chongqing Medical University. All surgeries were performed under anesthesia, and all efforts were made to minimize animal discomfort and stress.

Animals and experimental procedures: Female *BALB/c* mice at the age of 6 to 8 weeks were purchased from Jackson Laboratories (Bar Harbor, ME) and were housed under specific pathogen-free conditions at the Animal Care Service of Chongqing Medical University with a 12 h:12 h light-dark cycle. The mice were randomly divided into two groups: the LPS group and the control group. For the LPs group, to induce EIU, each mouse eye received a single intravitreal injection of 125 ng LPS prepared in 1 µl sterile PBS (140 mM NaCl, 2.7 mM KCl, 10 mM Na_2HPO_4, 2 mM KH_2PO_4, PH 7.4) as previously described [23]. For the control group, each mouse eye was given an injection of 1 µl sterile PBS.

Inflammation evaluation in the anterior chamber: Inflammation in the anterior chamber was evaluated with a slit-lamp (Shangbang, Chongqing, China) observation at the 24th hour after LPS administration. The mice were euthanized by receiving an intraperitoneal injection with the mixture of 75 mg/kg (ketamine) and 13.6 mg/kg (xylazine). The clinical severity of ocular inflammation was graded by two independent observers according to criteria described previously [23]. The clinical severity of ocular inflammation was graded according to the severity of iris hyperemia, exudate in anterior chamber, hypopyon and synechia by two independent observers according to the criteria described previously.

Histological evaluation: To evaluate the histological changes in the posterior segment, the eyes of the mice were then enucleated at the 24th hour after LPS injection and fixed in 4% paraformaldehyde (PFA) at 4 °C overnight. Eyeballs were embedded in paraffin. Serial 4 µm sections were cut through the cornea-optic nerve axis and stained with hematoxylin and eosin (H&E). Then the infiltrating cells in the posterior chamber and the retina were examined under a light microscope.

Library preparation and mRNA sequencing: The RNA-sequencing were performed by Novogene (Beijing, China). The library was prepared for sequencing using standard Illumina protocols. Total RNAs were isolated from the retinas of the LPS group and the control group using TRIzol reagent (Invitrogen, Carlsbad, CA) and treated with RNase-free DNase I (New England Biolabs, Ipswich, MA), to remove any contaminating genomic DNA. A total amount of 3 µg RNA per sample was used as input material for the RNA sample preparations. Sequencing libraries were generated using the NEBNext® Ultra™ RNA Library Prep Kit for Illumina® (New England Biolabs) following the manufacturer's instruction. mRNA extraction was performed using Dynabeads oligo (dT; Invitrogen Dynal). Double-stranded cDNAs were synthesized using Superscript II reverse transcriptase (Invitrogen) and random hexamer primers. The cDNAs were

then fragmented with nebulization, and the standard Illumina protocol was followed thereafter to create the RNA-seq library. The library quality was assessed with an Agilent 2100 Bioanalyzer (Agilent Technologies, Palo Alto, CA). The cDNA libraries were sequenced by the Illumina Hiseq 2500 device. For the data analysis, base calls were performed using CASAVA. Reads were aligned to the genome using the split read aligner TopHat (v2.0.12) with the mismatches set at 2 and with the default parameters.

Differentially expressed gene analysis: Differentially expressed gene (DEG) analysis of the LPS group and the control group (each group has three biologic replicates per condition) was performed using the DESeq R package (1.10.1). DESeq provides statistical routines for determining differential expression in digital gene expression data using a model based on the negative binomial distribution. The p values were adjusted using the Benjamini and Hochberg approach for controlling the false discovery rate (FDR). Genes with an adjusted p value of less than 0.05 found by DESeq were assigned as differentially expressed.

GO and KEGG pathways enrichment analysis of differentially expressed genes: Gene Ontology (GO) enrichment analysis of the DEGs was performed by the GOseq R package, in which gene length bias was corrected. GO terms with a corrected p value of less than 0.05 were considered significantly enriched by differential expressed genes. Pathway enrichment was determined using the Kyoto Encyclopedia of Genes and Genomes (KEGG) pathway annotation. KEGG is a database resource for understanding high-level functions and utilities of the biologic system, such as the cell, the organism, and the ecosystem, from molecular-level information, especially large-scale molecular data sets generated by genome sequencing and other high-through put experimental technologies (KEGG). We used KOBAS software (v 2.0) to test the statistical enrichment of differential expression genes in the KEGG pathways. Pathways were considered significantly enriched with an adjusted p value of less than 0.05.

Real-time quantitative PCR: Mice were euthanized at the 24th hour after LPS injection, and the retinas were freshly microdissected under a dissecting microscope to separate the neuroretina and the RPE-choroid complex. Total RNA of the neuroretina was then extracted using TRIzol reagent (Invitrogen) according to the manufacturer's instructions. cDNA was synthesized by using the PrimeScript RT reagent kit (Takara Biotechnology, Dalian, China). Real-time PCR analysis of IRF8 was performed in a volume of 20 µl using SYBR Premix Ex Taq™ II (Takara Biotechnology) with the ABI Prism 7500 system (Applied Biosystems, Foster City, CA). The conditions were 95 °C for 10 min, followed by 40 cycles of 15 s at 95 °C and 60 s at 60 °C. Each reaction was run in duplicate. Data were normalized to the expression of GAPDH. Relative quantification was achieved with the comparative $2^{-\Delta\Delta Ct}$ method as described previously [23]. The sequences of the PCR primer pairs used in this study are shown in Table 1.

Statistical analysis: Data are shown as mean±standard error of the mean (SEM). Real-time PCR data were analyzed with GraphPad Prism 5 software (GraphPad Software, Inc., San Diego, CA). The statistical significance of differences was determined with the independent-sample *t* test. A p value of less than 0.05 was considered statistically significant.

Table 1. Sequences of the primers for real-time PCR.

Gene	Accession number	Forward	Reverse
Ccl5	NM_013653.3	5′-CTGCTGCTTTGCCTACCTCT-3′	5′-ACACACTTGGCGGTTCCTT-3′
A2m	NM_175628.3	5′-TCTGCCTACATCACCATTGC-3′	5′-CTCTCCTCGCTGACTTCCAG-3′
Jak3	NM_001190830.1	5′-TGCCATCCTTGACTTACACG-3′	5′-GGAACTCTCCCTGCTCCTTC-3′
Egr1	NM_007913.5	5′-AACACTTTGTGGCCTGAACC-3′	5′-AGGCAGAGGAAGACGATGAA-3′
Atf3	NM_007498.3	5′-CCAGGTCTCTGCCTCAGAAG-3′	5′-GATGGCGAATCTCAGCTCTT-3′
Cdkn1a	NM_001111099.2	5′-CAAAGTGTGCCGTTGTCTCTT-3′	5′-TCAAAGTTCCACCGTTCTCG-3′
Gadd45b	NM_008655.1	5′-GTCGTTCTGCTGCGACAAT-3′	5′-TGACAGTTCGTGACCAGGAG-3′
C1ra	NM_023143.3	5′-CTGGAAGCTGCACTACACCA-3′	5′-TGAAGTAATCCCGGAACTGG-3′
Sell	XM_006496718.3	5′-CCAGTCCAAGTGTGCTTTCA-3′	5′-TCTCTTGGCAGATTGGCTCT-3′
C3	NM_009778.3	5′-TGGTGGAGAAAGCAGTGATG-3′	5′-ACGGGCAGTAGGTTGTTGTC-3′
F13a1	NM_001166391.1	5′-GCCCAATAACTCCAATGCTG-3′	5′-CCCATCTCTCCTTGAACAGG-3′
GAPDH	XM_017321385.1	5′-GTATGACTCCACTCACGGCAAA-3′	5′-GGTCTCGCTCCTGGAAGATG-3′

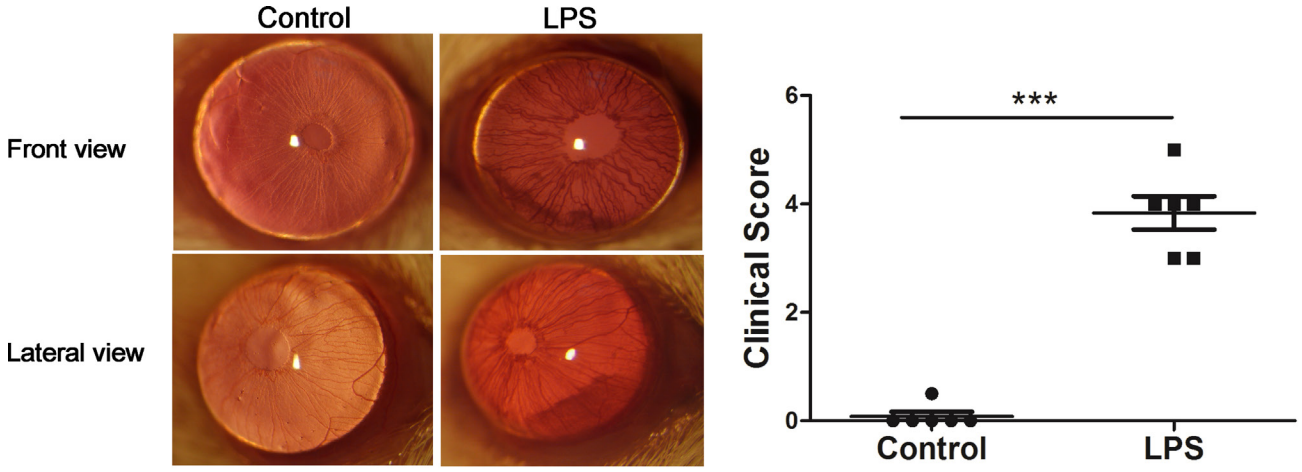

Figure 1. Inflammatory signs in the anterior chamber after LPS administration. The ocular inflammation was assessed with slit-lamp microscopy at the 24th hour after lipopolysaccharide (LPS) injection. **Left panel**: Representative images of the anterior chamber from the control- and LPS-treated groups at the 24th hour after the LPS injection. **Right panel**: The clinical score of the anterior chamber were evaluated at the 24th hour after LPS administration using the criteria of the endotoxin-induced uveitis (EIU) clinical score. The clinical score of ocular inflammation was assessed by two independent observers according to the criteria (n = 6).

RESULTS

Inflammation signs and clinical scores of the anterior chamber: Inflammation in the anterior chamber was assessed with a slit-lamp at 24 hours after LPS injection. The clinical scores were evaluated based on the criteria described previously [23] simultaneously with the slit-lamp. There was significant iris hyperemia and exudation into the anterior chamber, and hypopyon was observed in the LPS group. No inflammation was observed in the control group at the 24th hour. Evaluation of the clinical score showed that at the 24th hour, the clinical score for the mice in the LPS group was statistically significantly higher (3.83±0.75, mean ± SD) than that for the control group (0.08±0.20, mean ± SD; ***p<0.001; Figure 1).

Histological changes in the posterior chamber: To evaluate the histological changes, eyes were collected at the 24th hour after LPS injection. Histological examination showed that no inflammatory cells had infiltrated into the ciliary body or the vitreous cavity in the control group (Figure 2A,C). However, severe intraocular inflammation was observed in the LPS group as evidenced by a large number of inflammatory cells infiltrated into the vitreous cavity and the ciliary body (Figure 2B,D).

Hierarchical cluster of global gene expression: To examine the global gene expression in the LPS-treated tissue and the control retinal tissue, mRNA was extracted from three individual biologic replicates, and RNA-seq was performed. To compare the difference in the global gene expression profiles of the different samples, average linkage hierarchical cluster analysis was performed (Figure 3). The LPS-treated retina samples clearly separated from the control retina samples, suggesting that there is a distinct difference in gene expression between control and LPS-treated retinas.

DEGs in the retinas of the EIU mice and the control mice: To investigate the changes in gene expression after LPS administration, computational analysis of the DEGs between the LPS group and the control group was performed. Genes were considered to be differentially expressed with an adjusted p value of less than 0.05. A total of 478 genes exhibited altered expression in the LPS group versus the control group. Among these DEGs, 406 (85%) genes were upregulated in the LPS group (Figure 4, red dots; Appendix 1), and 72 genes (15%) were downregulated (Figure 4, green dots; Appendix 2).

GO enrichment analysis of DEGs: To investigate the GO, including the biological process, molecular function, and cellular location of the differentially expressed genes, GO enrichment analysis was applied to analyze all the DEGs in the LPS group compared with the control group. The top 30 most enriched upregulated and the top 30 most enriched downregulated GO terms are shown in Figure 5. The adjusted p values of the three upregulated GO terms were less than 0.05; thus, these GO terms were considered significantly enriched GO terms, including antigen processing and presentation, immune response, and immune system process (Table 2). These significantly upregulated GO terms were heavily associated with immune-related GO terms, indicating there was an increase in the immune response in the LPS-treated

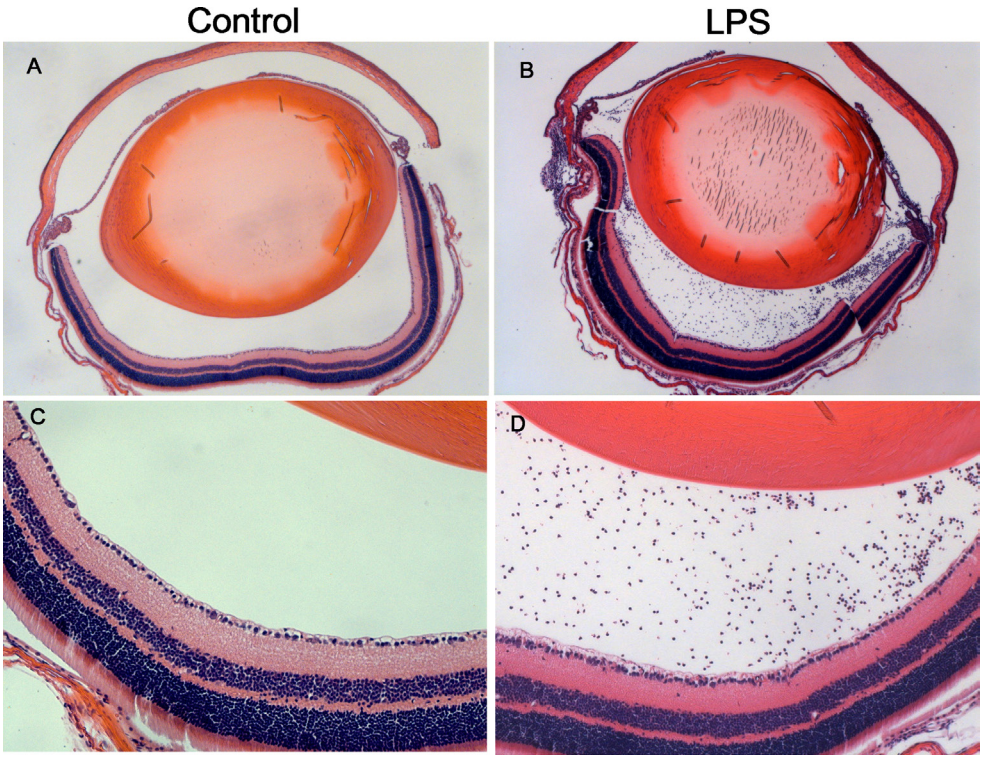

Figure 2. Histological evaluation of the eyes from the mice treated with or without LPS. Representative images (**A**, **C**) show infiltrating inflammatory cells in the posterior chamber of the eyes in the control group at the 24th hour. Representative images (**B**, **D**) show infiltrating inflammatory cells in the posterior chamber of the eyes in the lipopolysaccharide (LPS) group at the 24th hour after LPS injection. Magnification = 10X for **A** and **B** and 200X for **C** and **D** (n = 3).

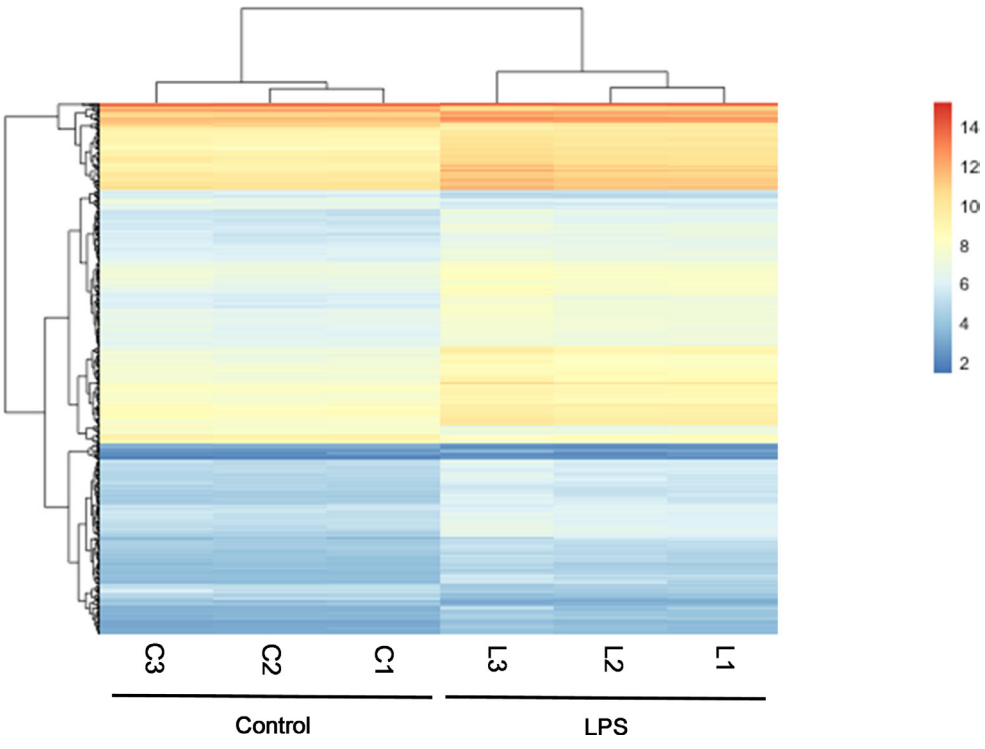

Figure 3. Hierarchical cluster analysis of the retinas between the EIU mice and the control mice. The cluster analysis displays gene expression changes in the retinas of the lipopolysaccharide (LPS)-treated mice and the control mice. Gene expression profiles of the control mice that received sham injection with PBS in each eye (C1–3, n = 3) were compared with the endotoxin-induced uveitis (EIU) mice that received a single intravitreal injection with LPS in each eye (L1–3, n = 3). Red bars indicate increased expression, and blue bars indicate decreased expression.

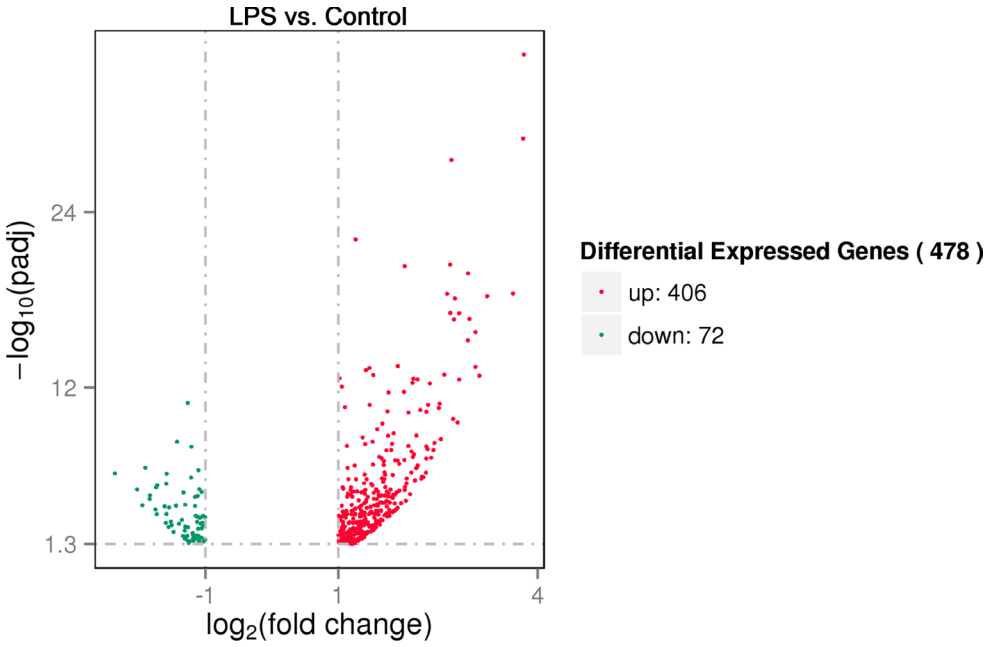

Figure 4. Volcano plot of the upregulated and downregulated DEGs. The volcano plot shows the upregulated and downregulated differentially expressed genes (DEGs) of the retinas in the lipopolysaccharide (LPS) group and the control group. For each plot, the x-axis represents the $\log_2$ fold change (FC), and the y-axis represents $-\log_{10}$ (p values). Genes with an adjusted p value of less than 0.05 found with DESeq were assigned as differentially expressed.

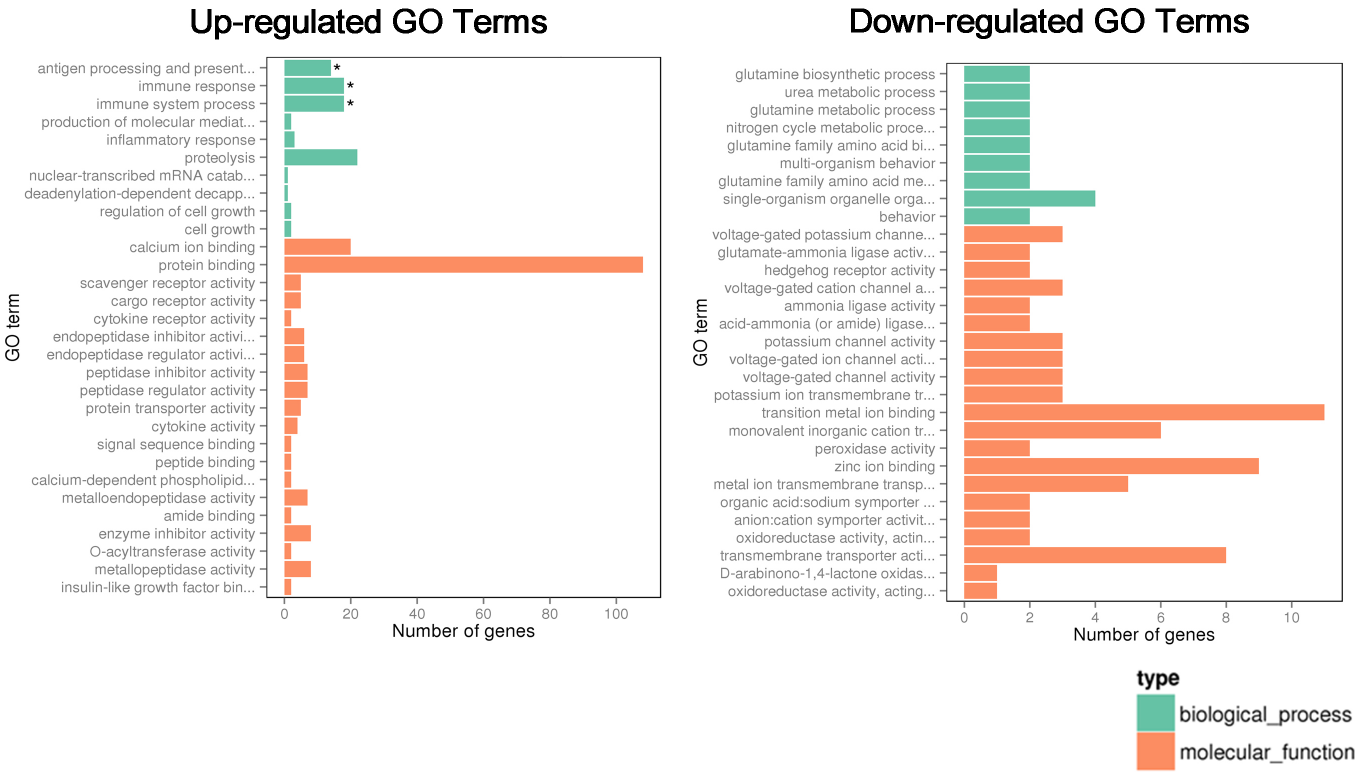

Figure 5. The top 30 enriched upregulated and the top 30 enriched downregulated GO terms in the LPS group compared with the control group. The top 30 upregulated and the top 30 downregulated Gene Ontology (GO) terms in the lipopolysaccharide (LPS) group compared to the control group. Enriched GO terms with an adjusted p value of less than 0.05 were considered significantly enriched (*adjusted p<0.05).

Table 2. The significantly enriched GO terms.

Up/down-regulated	GO accession	Description	Term type	Adjusted *p*-value
Upregulated GO Terms	GO:0019882	antigen processing and presentation	biologic process	3.38E-08
	GO:0006955	immune response	biologic process	3.11E-05
	GO:0002376	immune system process	biologic process	7.81E-05

retinas. No significantly downregulated GO terms were enriched (Figure 5).

KEGG pathway analysis of DEGs in the LPS group compared with the control group: To identify the pathways involved in EIU, KEGG pathway enrichment analysis were applied. The top 20 upregulated pathways and the top 20 downregulated pathways are shown in Figure 6. A total of 21 significantly enriched upregulated pathways were found, including phagosome, viral myocarditis, staphylococcus aureus infection, herpes simplex infection, HTLV-I infection, allograft rejection, graft-versus-host disease, type I diabetes mellitus, viral carcinogenesis, autoimmune thyroid disease, complement and coagulation cascades, antigen processing and presentation, Epstein-Barr virus infection, cell adhesion molecules (CAMs), measles, osteoclast differentiation, Chagas disease (American trypanosomiasis), legionellosis, pertussis, the p53 signaling pathway, and the tumor necrosis factor (TNF) signaling pathway. Six significantly downregulated pathways were enriched, including platelet activation, nitrogen metabolism, gastric acid secretion, bacterial invasion of epithelial cells, protein digestion and absorption, and glyoxylate and dicarboxylate metabolism (Table 3).

Validation of the DEGs with real-time PCR: To validate the DEGs from the RNA-seq findings, we prepared new mouse retinas in each group and performed real-time PCR. A total of 11 genes (log_2 fold change >2 and adjusted p<0.05) from the significantly enriched GO terms and KEGG pathways were chosen to be validated. The chosen genes are shown in Table 4. The chosen genes that met the criteria were all upregulated in the LPS-treated group according to the RNA-seq results. The validated genes were chosen from the significantly enriched GO terms, including immune response and immune system process. These genes were also involved in 21 significantly upregulated enriched KEGG pathways, including phagosome,

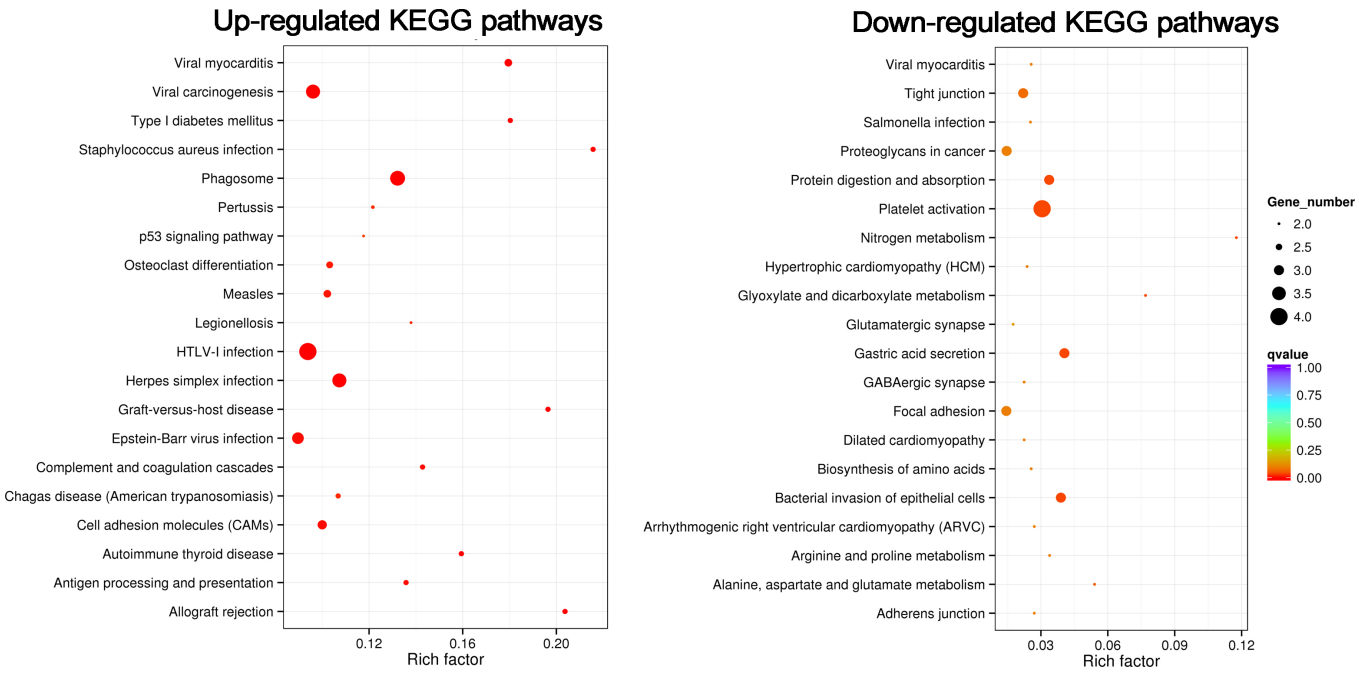

Figure 6. The top 20 enriched upregulated and the top 20 enriched downregulated KEGG pathways in the LPS group compared with the control group. The top 20 upregulated and the top 20 downregulated Kyoto Encyclopedia of Genes and Genomes (KEGG) pathways of the differentially expressed genes (DEGs) in the lipopolysaccharide (LPS) group compared with the control group. Enriched pathways with an adjusted p value of less than 0.05 were considered significantly enriched (*adjusted p<0.05).

Table 3. The significantly enriched KEGG pathways.

Up/down-regulated	ID	Pathway terms	P-Value	Corrected P-Value
Upregulated pathways	mmu04145	Phagosome	1.15E-07	2.10E-05
	mmu05416	Viral myocarditis	1.48E-06	0.000135509
	mmu05150	Staphylococcus aureus infection	4.24E-06	0.000208759
	mmu05168	Herpes simplex infection	5.03E-06	0.000208759
	mmu05166	HTLV-I infection	6.82E-06	0.000208759
	mmu05330	Allograft rejection	6.84E-06	0.000208759
	mmu05332	Graft-versus-host disease	9.27E-06	0.000242254
	mmu04940	Type I diabetes mellitus	1.88E-05	0.000430529
	mmu05203	Viral carcinogenesis	2.46E-05	0.000500679
	mmu05320	Autoimmune thyroid disease	5.16E-05	0.000944675
	mmu04610	Complement and coagulation cascades	0.0001248	0.002076447
	mmu04612	Antigen processing and presentation	0.0001865	0.002621852
	mmu05169	Epstein-Barr virus infection	0.0001981	0.002621852
	mmu04514	Cell adhesion molecules (CAMs)	0.0002006	0.002621852
	mmu05162	Measles	0.0004025	0.004910452
	mmu04380	Osteoclast differentiation	0.0005894	0.006741672
	mmu05142	Chagas disease (American trypanosomiasis)	0.0011778	0.012678867
	mmu05134	Legionellosis	0.0012619	0.012828809
	mmu05133	Pertussis	0.0014304	0.013776561
	mmu04115	p53 signaling pathway	0.003126	0.028603336
	mmu04668	TNF signaling pathway	0.0052882	0.04608275
Downregulated pathways	mmu04611	Platelet activation	0.0012801	0.032394895
	mmu00910	Nitrogen metabolism	0.00197	0.032394895
	mmu04971	Gastric acid secretion	0.0024731	0.032394895
	mmu05100	Bacterial invasion of epithelial cells	0.002757	0.032394895
	mmu04974	Protein digestion and absorption	0.0040898	0.033425935
	mmu00630	Glyoxylate and dicarboxylate metabolism	0.0042671	0.033425935

viral myocarditis, staphylococcus aureus infection, herpes simplex infection, HTLV-I infection, allograft rejection, graft-versus-host disease, type I diabetes mellitus, viral carcinogenesis, autoimmune thyroid disease, complement and coagulation cascades, antigen processing and presentation, Epstein-Barr virus infection, cell adhesion molecules (CAMs), measles, osteoclast differentiation, Chagas disease (American trypanosomiasis), legionellosis, pertussis, the p53 signaling pathway, and the TNF signaling pathway. No DEGs met the criteria of a $\log_2$ fold-change greater than 2 and an adjusted p value of less than 0.05 in the significantly downregulated pathways. The 11 chosen genes can be divided into four groups: inflammatory response–related genes (*Ccl5*, *JAK3*, and *Sell*), complement system–related genes (*C1ra* and *C3*), fibrinolytic system–related genes (*F13a1* and *A2m*), and cell stress–related genes (*Cdkn1a*, *Gadd45b*, *Egr1*, and *Atf3*). We found that the results obtained with real-time PCR were in consistent with those obtained with RNA-seq. All the validated genes were significantly upregulated in the LPS group compared with the control group (*p<0.05, **p<0.01,***p<0.001; Figure 7).

DISCUSSION

In the present study, we identified a series of differentially expressed genes occurring in the retinal transcriptome of LPS-induced uveitis mice. We also attempted to identify relevant molecular pathways, with the goal of discovering potential therapeutic targets of uveitis. The results indicated that in addition to the inflammatory response, abnormal changes in complement system–, fibrinolytic system–, and

Table 4. Genes validated by real time PCR.

Ensgene	Symbol	log2 Fold Change	Adjusted p value	Description
ENSMUSG00000035042	Ccl5	3.780941071	9.15E-30	chemokine (C-C motif) ligand 5
ENSMUSG00000030111	A2m	2.741365525	2.14E-17	alpha-2-macroglobulin
ENSMUSG00000031805	Jak3	2.525753144	1.26E-11	Janus kinase 3
ENSMUSG00000038418	Egr1	2.235443805	3.43E-11	early growth response 1
ENSMUSG00000026628	Atf3	2.122053519	5.52E-08	activating transcription factor 3
ENSMUSG00000023067	Cdkn1a	2.19450178	2.16E-07	cyclin-dependent kinase inhibitor 1A (P21)
ENSMUSG00000015312	Gadd45b	2.179217262	3.03E-07	growth arrest and DNA-damage-inducible 45 beta
ENSMUSG00000055172	C1ra	2.171879166	3.30E-07	complement component 1, r subcomponent A
ENSMUSG00000026581	Sell	2.251491474	1.72E-06	selectin, lymphocyte
ENSMUSG00000024164	C3	2.15560777	2.24E-06	complement component 3
ENSMUSG00000039109	F13a1	2.01578419	5.52E-05	coagulation factor XIII, A1 subunit

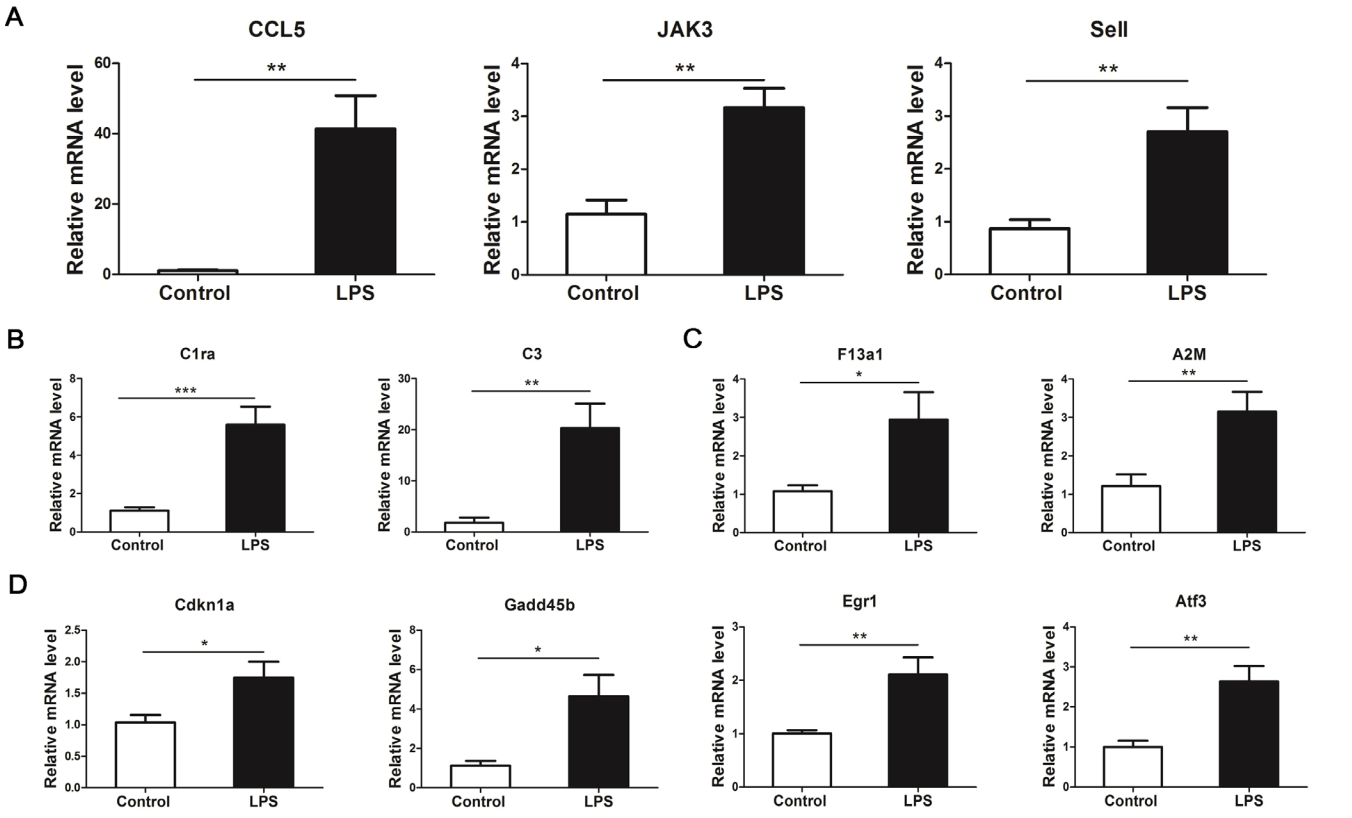

Figure 7. Validation of DEGs using real-time PCR. The validated genes were chosen from the significantly enriched Gene Ontology (GO) terms and the Kyoto Encyclopedia of Genes and Genomes (KEGG) pathway. The mRNA expression of inflammatory response–related genes (*Ccl5*, *JAK3*, and *Sell*; **A**), complement system–related genes (*C1ra* and *C3*; **B**), fibrinolytic system–related genes (*F13a1* and *A2m*; **C**), and cell stress–related genes (*Cdkn1a*, *Gadd45b*, *Egr1*, and *Atf3*; **D**) were remarkably higher in the lipopolysaccharide (LPS) group compared with the control group (*p<0.05, **p<0.01, ***p<0.001, n = 6).

cell stress–related genes may be involved in the pathogenesis of EIU. Treatment targeting these genes may assist in discovering novel therapeutic targets and finding candidate drugs.

The top five genes with the greatest fold changes include *Ccl5*, *A2m*, *Jak3*, *Egr1*, and *Atf3*. Ccl5 is a key inflammatory mediator of uveitis in animal models [24] and patients [25]. This mediator attracts mononuclear cells to the inflammatory site [26], allowing escalation of the inflammatory response in the ocular vasculature [27]. α2-macroglobulin (A2m) is a specific cytokine carrier that binds inflammatory cytokines implicated in LPS-induced inflammation [28] and has great potential to regulate cytokine homeostasis [29]. Janus kinase 3 (Jak3) plays an important role in the activation of cytokines during immune and inflammation responses [30]. Early growth response 1 (Egr1) is an important transcription factor for regulating the genes involved in inflammation, immunity, and coagulation [31]. Activating transcription factor 3 (Atf3) is a counter-regulatory immune transcription factor induced by Toll-like receptor (TLR) signaling [32]. Existing evidence showed these genes would be increased in response to LPS stimuli [24,33-36]. In parallel with previous studies, the present RNA-seq results showed the mRNA expression of these genes was significantly increased in response to LPS.

In general, the GO and KEGG pathway enrichment analysis of the RNA-seq data revealed that four types of genes were significantly upregulated, including the inflammatory response–related genes (*Ccl5*, *JAK3*, and *Sell*), complement system–related genes (*C1ra* and *C3*), fibrinolytic system–related genes (*F13a1* and *A2m*), and cell stress–related genes (*Cdkn1a*, *Gadd45b*, *Egr1*, and *Atf3*). Consistent with the well-accepted notion, we showed a remarkable increase in the inflammatory response–related genes: (*Ccl5*, *JAK3*, and *Sell*). Notably, we also found some complement system– and fibrinolytic system–related genes were increased in response to LPS, indicating that not only inflammatory response occurs during uveitis, but also the complement and fibrinolytic system may be involved in the pathogenesis of EIU. In addition, previous studies showed that a drug targeted to the fibrinolytic system plays a role in the regulation of coagulation and inflammation and may also regulate the complement systems in infectious gastroduodenal disease and sepsis-induced liver injury in mice [37,38], indicating that the inflammation, complement, and fibrinolytic systems may be closely related to and affect each other in the infectious inflammatory responses.

The present data suggested that abnormal changes in the inflammatory response–, complement system–, and fibrinolytic system–related genes happened concurrently during EIU and may be associated with the pathogenesis of LPS-induced uveitis. Additionally, candidate drugs that target the genes of these systems may provide better therapeutic strategies for treating patients who do not respond well to conventional drugs. However, the functional evidence of these DEGs needs to be proved in future work.

This study has several limitations. First, we analyzed transcriptional changes in the retinas at the 24th hour after LPS injection. The retinal RNA profile presented at this time point could likely not only be reflective of retina cells but also show what is occurring within the infiltrated cells. Samples collected at a single time point may not be enough to reveal the transcriptional changes involved in the development of EIU. Thus, dynamic transcriptome studies of EIU at different time points would provide more comprehensive knowledge. Moreover, the marked influx of blood cells within the posterior segment would also be included in this transcriptome profile. The transcripts derived from these cells cannot be excluded in this study. Therefore, further studies of retina samples treated with perfusion should exclude the influence of these infiltrated cells.

Taken together, the retinal transcriptomic analysis, which relied on RNA-seq, was an effective and comprehensive method for acquiring a global view of gene expression changes in the retina after the exposure to LPS. This study may provide new insights into the molecular mechanisms underlying LPS-induced ocular inflammation and may provide useful information toward discovering novel therapeutic targets for ocular inflammatory diseases.

APPENDIX 1. THE UP-REGULATED DEGS IN THE LPS GROUP COMPARED WITH THE CONTROL GROUP.

To access the data, click or select the words "Appendix 1."

APPENDIX 2. THE DOWN-REGULATED DEGS IN THE LPS GROUP COMPARED WITH THE CONTROL GROUP.

To access the data, click or select the words "Appendix 2."

ACKNOWLEDGMENTS

We are grateful for financial support from the National Natural Science Foundation of China grants (81,271,033, 81,470,621), Chongqing Science and Technology Commission (2014pt-sy10002) and National Key Clinical Specialties Construction Program of China. The authors alone are responsible for the content and writing of this article. Author contributions: Y. G. Q. and B. L. conceived the ideas and designed the experiments; Y. G. Q., P. Y., R. L., and X. Y. F.

performed all the experiments; Y. G. Q. and P. Y. analyzed all the data; Y. G. Q. wrote the manuscript; B. L. and B. T. H. reviewed and revised the manuscript. All authors read and approved the final version of the manuscript.

REFERENCES

1. Miserocchi E, Fogliato G, Modorati G, Bandello F. Review on the worldwide epidemiology of uveitis. Eur J Ophthalmol 2013; 23:705-17. [PMID: 23661536].
2. Read RW. Uveitis: advances in understanding of pathogenesis and treatment. Curr Rheumatol Rep 2006; 8:260-6. [PMID: 16839504].
3. Tabbara KF. Infectious uveitis: a review. Arch Soc Esp Oftalmol 2000; 75:215-59. [PMID: 11151155].
4. Munoz-Fernandez S, Martin-Mola E. Uveitis. Best Pract Res Clin Rheumatol 2006; 20:487-505. .
5. Gomes Bittencourt M, Sepah YJ, Do DV, Agbedia O, Akhtar A, Liu H, Akhlaq A, Annam R, Ibrahim M, Nguyen QD. New treatment options for noninfectious uveitis. Dev Ophthalmol 2012; 51:134-61. [PMID: 22517211].
6. Servat JJ, Mears KA, Black EH, Huang JJ. Biological agents for the treatment of uveitis. Expert Opin Biol Ther 2012; 12:311-28. [PMID: 22339439].
7. Rosenbaum JT, McDevitt HO, Guss RB, Egbert PR. Endotoxin-induced uveitis in rats as a model for human disease. Nature 1980; 286:611-3. [PMID: 7402339].
8. Akira S, Takeda K. Toll-like receptor signalling. Nat Rev Immunol 2004; 4:499-511. [PMID: 15229469].
9. Johnson GL, Lapadat R. Mitogen-activated protein kinase pathways mediated by ERK, JNK, and p38 protein kinases. Science 2002; 298:1911-2. .
10. Andonegui G, Zhou H, Bullard D, Kelly MM, Mullaly SC, McDonald B, Long EM, Robbins SM, Kubes P. Mice that exclusively express TLR4 on endothelial cells can efficiently clear a lethal systemic Gram-negative bacterial infection. J Clin Invest 2009; 119:1921-30. [PMID: 19603547].
11. Wang Z, Gerstein M, Snyder M. RNA-Seq: a revolutionary tool for transcriptomics. Nat Rev Genet 2009; 10:57-63. .
12. Margulies M, Egholm M, Altman WE, Attiya S, Bader JS, Bemben LA, Berka J, Braverman MS, Chen YJ, Chen Z, Dewell SB, Du L, Fierro JM, Gomes XV, Godwin BC, He W, Helgesen S, Ho CH, Irzyk GP, Jando SC, Alenquer ML, Jarvie TP, Jirage KB, Kim JB, Knight JR, Lanza JR, Leamon JH, Lefkowitz SM, Lei M, Li J, Lohman KL, Lu H, Makhijani VB, McDade KE, McKenna MP, Myers EW, Nickerson E, Nobile JR, Plant R, Puc BP, Ronan MT, Roth GT, Sarkis GJ, Simons JF, Simpson JW, Srinivasan M, Tartaro KR, Tomasz A, Vogt KA, Volkmer GA, Wang SH, Wang Y, Weiner MP, Yu P, Begley RF, Rothberg JM. Genome sequencing in microfabricated high-density picolitre reactors. Nature 2005; 437:376-80. [PMID: 16056220].
13. Schuster SC. Next-generation sequencing transforms today's biology. Nat Methods 2008; 5:16-8. [PMID: 18165802].
14. Mortazavi A, Williams BA, McCue K, Schaeffer L, Wold B. Mapping and quantifying mammalian transcriptomes by RNA-Seq. Nat Methods 2008; 5:621-8. [PMID: 18516045].
15. Wilhelm BT, Marguerat S, Watt S, Schubert F, Wood V, Goodhead I, Penkett CJ, Rogers J, Bahler J. Dynamic repertoire of a eukaryotic transcriptome surveyed at single-nucleotide resolution. Nature 2008; 453:1239-43. [PMID: 18488015].
16. Trapnell C, Williams BA, Pertea G, Mortazavi A, Kwan G, van Baren MJ, Salzberg SL, Wold BJ, Pachter L. Transcript assembly and quantification by RNA-Seq reveals unannotated transcripts and isoform switching during cell differentiation. Nat Biotechnol 2010; 28:511-5. [PMID: 20436464].
17. Brooks MJ, Rajasimha HK, Roger JE, Swaroop A. Next-generation sequencing facilitates quantitative analysis of wild-type and Nrl(−/−) retinal transcriptomes. Mol Vis 2011; 17:3034-54. [PMID: 22162623].
18. Kandpal RP, Rajasimha HK, Brooks MJ, Nellissery J, Wan J, Qian J, Kern TS, Swaroop A. Transcriptome analysis using next generation sequencing reveals molecular signatures of diabetic retinopathy and efficacy of candidate drugs. Mol Vis 2012; 18:1123-46. [PMID: 22605924].
19. Mustafi D, Maeda T, Kohno H, Nadeau JH, Palczewski K. Inflammatory priming predisposes mice to age-related retinal degeneration. J Clin Invest 2012; 122:2989-3001. [PMID: 22797304].
20. Swaroop A, Zack DJ. Transcriptome analysis of the retina. Genome Biol. 2002;3:REVIEWS1022.
21. Blackshaw S, Fraioli RE, Furukawa T, Cepko CL. Comprehensive analysis of photoreceptor gene expression and the identification of candidate retinal disease genes. Cell 2001; 107:579-89. [PMID: 11733058].
22. Hackam AS, Qian J, Liu D, Gunatilaka T, Farkas RH, Chowers I, Kageyama M, Parmigiani G, Zack DJ. Comparative gene expression analysis of murine retina and brain. Mol Vis 2004; 10:637-49. [PMID: 15359217].
23. Qiu Y, Shil PK, Zhu P, Yang H, Verma A, Lei B, Li Q. Angiotensin-converting enzyme 2 (ACE2) activator diminazene aceturate ameliorates endotoxin-induced uveitis in mice. Invest Ophthalmol Vis Sci 2014; 55:3809-18. [PMID: 24854854].
24. Smith JR, Hart PH, Williams KA. Basic pathogenic mechanisms operating in experimental models of acute anterior uveitis. Immunol Cell Biol 1998; 76:497-512. [PMID: 9893027].
25. Verma MJ, Lloyd A, Rager H, Strieter R, Kunkel S, Taub D, Wakefield D. Chemokines in acute anterior uveitis. Curr Eye Res 1997; 16:1202-8. [PMID: 9426952].
26. Laubli H, Spanaus KS, Borsig L. Selectin-mediated activation of endothelial cells induces expression of CCL5 and promotes metastasis through recruitment of monocytes. Blood 2009; 114:4583-91. [PMID: 19779041].

27. Bellingan G. Leukocytes: friend or foe. Intensive Care Med 2000; 26:Suppl 1S111-8. [PMID: 10786967].

28. Gourine AV, Gourine VN, Tesfaigzi Y, Caluwaerts N, Van Leuven F, Kluger MJ. Role of alpha(2)-macroglobulin in fever and cytokine responses induced by lipopolysaccharide in mice. Am J Physiol 2002; 283:R218-26. [PMID: 12069948].

29. Gonias SL, LaMarre J, Crookston KP, Webb DJ, Wolf BB, Lopes MB, Moses HL, Hayes MA. Alpha 2-macroglobulin and the alpha 2-macroglobulin receptor/LRP. A growth regulatory axis. Ann N Y Acad Sci 1994; 737:273-90. [PMID: 7524402].

30. Ghoreschi K, Laurence A, O'Shea JJ. Janus kinases in immune cell signaling. Immunol Rev 2009; 228:273-87. [PMID: 19290934].

31. Pritchard MT, Nagy LE. Ethanol-induced liver injury: potential roles for egr-1. Alcohol Clin Exp Res 2005; 29:146S-50S. [PMID: 16344600].

32. Gilchrist M, Thorsson V, Li B, Rust AG, Korb M, Roach JC, Kennedy K, Hai T, Bolouri H, Aderem A. Systems biology approaches identify ATF3 as a negative regulator of Toll-like receptor 4. Nature 2006; 441:173-8. [PMID: 16688168].

33. Lyoumi S, Puy H, Tamion F, Bogard C, Leplingard A, Scotte M, Vranckx R, Gauthier F, Hiron M, Daveau M, Nordmann Y, Deybach JC, Lebreton JP. Heme and acute inflammation role in vivo of heme in the hepatic expression of positive acute-phase reactants in rats. Eur J Biochem 1999; 261:190-6. [PMID: 10103050].

34. Verbsky JW, Bach EA, Fang YF, Yang L, Randolph DA, Fields LE. Expression of Janus kinase 3 in human endothelial and other non-lymphoid and non-myeloid cells. J Biol Chem 1996; 271:13976-80. [PMID: 8662778].

35. Guillem-Llobat P, Iniguez MA. Inhibition of lipopolysaccharide-induced gene expression by liver X receptor ligands in macrophages involves interference with early growth response factor 1. Prostaglandins Leukot Essent Fatty Acids 2015; 96:37-49. [PMID: 25736222].

36. Shan Y, Akram A, Amatullah H, Zhou DY, Gali PL, Maron-Gutierrez T, Gonzalez-Lopez A, Zhou L, Rocco PR, Hwang D, Albaiceta GM, Haitsma JJ, dos Santos CC. ATF3 protects pulmonary resident cells from acute and ventilator-induced lung injury by preventing Nrf2 degradation. Antioxid Redox Signal 2015; 22:651-68. .

37. Ikeda A, Gabazza EC, Morser J, Imoto I, Kuroda M, D'Alessandro-Gabazza CN, Hara K, Ruiz DB, Bernabe PG, Katsurahara M, Toda M, Kobayashi Y, Yano Y, Sumida Y, Suzuki K, Taguchi O, Takei Y. Presence of thrombin-activatable fibrinolysis inhibitor in Helicobacter pylori-associated gastroduodenal disease. Helicobacter 2009; 14:147-55. [PMID: 19298343].

38. Renckens R, Roelofs JJ, ter Horst SA, van 't Veer C, Havik SR, Florquin S, Wagenaar GT, Meijers JC, van der Poll T. Absence of thrombin-activatable fibrinolysis inhibitor protects against sepsis-induced liver injury in mice. J Immunol 2005; 175:6764-71. [PMID: 16272333].

Articles are provided courtesy of Emory University and the Zhongshan Ophthalmic Center, Sun Yat-sen University, P.R. China. The print version of this article was created on 3 July 2017. This reflects all typographical corrections and errata to the article through that date. Details of any changes may be found in the online version of the article.